Genome-Wide Identification and Stress-Responsive Expression Analysis of the Actin-Depolymerizing Factor (ADF) Gene Family in Avena sativa L

Deying Wang
Chinese Academy of Sciences
Tao Liu
Chinese Academy of Sciences
Wenhui Tian
Chinese Academy of Sciences
Hong Chen
Chinese Academy of Sciences
Guoqing Wang
Chinese Academy of Sciences
Bo Zhang
zhangbo@nwipb.cas.cn

Chinese Academy of Sciences

Research Article

Keywords: actin-depolymerizing factor, oat, circadian rhythm, abiotic stresses, expression analysis

Posted Date: December 18th, 2025

DOI: https://doi.org/10.21203/rs.3.rs-8235971/v1

Additional Declarations: No competing interests reported.

Version of Record: A version of this preprint was published at BMC Plant Biology on February 9th, 2026. See the published version at https://doi.org/10.1186/s12870-026-08329-9.

Abstract

Background

Oat (*Avena sativa* L.) is an important cereal crop globally, valued for both its grain and forage. Actin depolymerization factors (ADFs) are highly conserved eukaryotic proteins that facilitate remodeling of the actin cytoskeleton. Accumulating evidence indicates that *ADFs* play crucial roles in plant growth, development, and stress responses. Nevertheless, the *AsADFs* family has not yet been identified in oat, an important cereal with high abiotic stress tolerance.

Results

In this study, a total of 18 *ADF* genes (*AsADF*) were identified from the oat reference genome (Sang.v1.1) and mapped to 12 different chromosomes. Based on the phylogenetic analysis, these genes were classified into four groups, which was confirmed by their structure and the distribution of conserved motifs in the encoded proteins. Collinearity analysis demonstrated strong relationships between oat and wheat *ADFs*. The promoters of most *AsADFs* family contain cis-elements associated with growth, development, and stress responses, suggesting their potential involvement in these biological processes. Subcellular localization prediction indicated that ADFs are mainly located in the cytoplasm, and this localization is consistent with their role in cytoskeletal maintenance. Analysis of qRT-PCR results indicated that most *AsADFs* exhibited differential expression patterns under circadian rhythm and responded to various abiotic stresses. Among them, the expression levels of *AsADF9*, *13*, and *14* from group B showed significant changes under all four abiotic stress conditions, suggesting their important roles in abiotic stress resistance.

Conclusions

This study revealed that *AsADF* genes play crucial roles in oat's response to various abiotic stresses. Notably, the expression of *AsADF9*, *13* and *14* was strongly induced under stress conditions, highlighting them as key candidates mediating oat's stress response. In summary, the present study established a theoretical foundation for analyzing the molecular mechanism of stress resistance in oat and provides valuable insights for molecular breeding to enhance stress resistance.

Background

The actin-based microfilament cytoskeleton is essential for numerous cellular processes, providing mechanical support and motive force for the cell, and playing critical roles in plant growth, development, and stress responses [1–3]. Actin exists in two forms: globular actin (G-actin) and filamentous actin (F-actin) [4]. The polymerization of G-actin into F-actin enables a wide range of biological functions [5, 6]. The remodeling of F-actin is driven by a diverse set of actin-binding proteins (ABPs), which in turn regulate various cellular and physiological functions [7, 8]. Among these, the actin depolymerizing factor (ADF) represents a crucial ABP that severs and depolymerizes F-actin [9, 10].

The number of *ADF* family genes varies considerably among different organisms. Most non-plant organisms have only one or two ADF/cofilin genes. In contrast, plants typically possess an expanded ADF family, which enables them to fulfill diverse physiological functions [5, 11]. Given the important functions of the actin cytoskeleton in plant development and stress responses, ADF proteins are regulators of cellular processes [5, 9]. Consequently, genome-wide identification and functional characterization of the *ADF* family have been performed in numerous plant species (Table S1).

The *ADF* gene family plays crucial roles in plant growth and development, and the functional characterization of *ADFs* has been conducted in various plant species. For instance, in *Arabidopsis thaliana*, the *atadf9* mutant displays reduced lateral branches and diminished callus-forming capacity [12]. *AtADF1* and *AtADF4* promote hypocotyl elongation by interacting with 14-3-3 λ proteins [13, 14]. *AtADF7* and *AtADF10* regulate pollen tube growth by modulating cytosolic pH [15]. Beyond A. *thaliana*, studies in cotton have shown that suppressing *GhADF1* expression enhances both fiber elongation and secondary cell wall deposition [16]. In maize, *ZmADF1* is pollen-specific and negatively regulates pollen quantity, viability, germination, and seed set [17]. Beyond growth, *ADFs* are crucial for stress responses. The *atadf5* mutant exhibits reduced drought survival due to impaired stomatal closure [18]. *AtADF1* responds to salt stress via its association with MYB73 [19], while *AtADF4* confers osmotic stress tolerance [14]. *GhADF6* is implicated in the response to *Verticillium dahliae* [20]. Heterologous expression of *GmADF13* in *Arabidopsis* and soybean hairy roots enhances drought tolerance [21]. Overexpression of *OsADF3* also improves drought tolerance in transgenic *A. thaliana* seedlings [22]. *ZmADF1* plays a critical role in regulating growth under high-temperature stress [11]. In wheat, *TaADF3* negatively regulates *Puccinia striiformis* (PST) resistance, likely by modulating ROS homeostasis [23]. In contrast, *TaADF4* and *TaADF7* are shown to confer resistance to PST by remodeling the actin cytoskeleton [24, 25]. Furthermore, heterologous overexpression of *TaADF16* is shown to enhance cold tolerance in transgenic *A. thaliana* by boosting ROS scavenging capacity [26].

As the world's seventh most widely grown cereal crop, oat (*Avena sativa* L.) is a valuable cultivated dual-purpose species [27–29]. This health-promoting cereal has garnered increasing attention due to its rich content of dietary fiber, phytochemicals, and essential nutrients [30, 31]. Concurrently, as a crucial forage crop, oat provides high-quality feed for livestock. This helps alleviate pressure on conventional feed grains and natural grasslands, thereby facilitating the restoration of degraded pastures and ecological conservation [32, 33]. Oats not only possess significant economic value but are also considered a valuable gene pool due to their tolerance to stress conditions. Oat contains numerous stress-resistance genes yet to be discovered, which can provide vital resources for crop stress-resistance improvement. Stable yield is crucial for oat production. Despite oat’s considerable ability to tolerate environmental stresses, their growth and development are still affected by various stresses, such as extreme temperatures, cold, and drought, leading to substantial yield losses [34–36].

In this study, 18 *AsADF* genes were identified from the oat Sang reference genome (Sang.v1.1) and a comprehensive analysis was conducted. Initially, we assessed their fundamental physicochemical properties and chromosomal locations. To elucidate their evolutionary relationships, we constructed a phylogenetic tree and analyzed the protein structures. Furthermore, cis-elements within the promoter regions were predicted, along with their subcellular localization. Finally, to investigate their potential regulatory mechanisms and functions, we examined their expression patterns under circadian rhythms and their expression level changes

under abiotic stress. This study establishes a foundation for screening key candidate genes within the *ADF* family in oats and provides valuable genetic resources for molecular breeding aimed at stress resistance.

Results

Identification of *ADF* genes in oat

Through a comprehensive analysis of the ADF-H domain (PF00241) annotation and the CD-Search tool from the National Center for Biotechnology Information (NCBI) (https://www.ncbi.nlm.nih.gov/cdd/), a total of 18 putative *ADF* genes were identified in the oat genome. These genes were located on 12 different chromosomes and were designated AsADF1 to AsADF18 based on their respective gene IDs in the Sang reference genome (Table 1, Fig. 1).

Analysis of the basic physicochemical properties of AsADF proteins revealed substantial variation among members. Their amino acid lengths ranged from 139 aa (AsADF4, 5, 6, 7, and 17) to 152 aa (AsADF1). The molecular weight (MW) varied between 15.75 kDa (AsADF13) and 17.30 kDa (AsADF1), and the theoretical isoelectric point (pI) spanned from 4.43 (AsADF13) to 8.73 (AsADF2 and AsADF6). The instability index (InI) ranged from 31.61 (AsADF6) to 47.73 (AsADF17), while the aliphatic index (AI) values between 61.08 (AsADF6) and 85.65 (AsADF14) suggest relatively high thermal stability. Finally, the grand average of hydropathicity (GRAVY) scores ranged from -0.037 (AsADF17) to -0.567 (AsADF4), indicating that all these proteins are hydrophilic (Table 1).

Subcellular localization predictions indicated that the ADF proteins are mainly localized in the cytoplasm, followed by the chloroplast, nucleus, extracellular space, mitochondria, and peroxisomes. This distribution implies potential functional roles for ADF proteins within these organelles (Fig. S1).

Table 1 Physicochemical properties of AsADF proteins in oats

Sequence ID	Name	Protein Length	MW(kDa)	pI	InI	AI	GRAVY
AVESA.00010b.r2.1AG0061340.1	AsADF1	152	17307.39	5.22	45.64	74.47	-0.493
AVESA.00010b.r2.1DG0136740.1	AsADF2	143	16402.91	8.73	43.25	74.34	-0.3
AVESA.00010b.r2.1DG0179840.1	AsADF3	150	17278.35	5.1	44.51	72.13	-0.541
AVESA.00010b.r2.2AG0200070.1	AsADF4	139	16043.09	5.4	36.85	63.24	-0.567
AVESA.00010b.r2.2CG0312780.1	AsADF5	139	15755.91	5.55	43.77	61.8	-0.439
AVESA.00010b.r2.2DG0370090.1	AsADF6	139	15885.01	5.25	31.61	61.08	-0.488
AVESA.00010b.r2.3DG0568620.1	AsADF7	139	15931.18	5.52	42.74	77.91	-0.376
AVESA.00010b.r2.4AG0610360.1	AsADF8	145	16778.06	5.94	42.93	72.69	-0.44
AVESA.00010b.r2.4AG0615680.1	AsADF9	147	15789.71	4.64	39.33	83.67	-0.059
AVESA.00010b.r2.4AG0615690.1	AsADF10	142	16055.08	5.46	44.36	74.23	-0.484
AVESA.00010b.r2.4CG1327640.1	AsADF11	143	16416.94	8.73	45.53	74.34	-0.3
AVESA.00010b.r2.4DG0753700.1	AsADF12	145	16720.02	6.31	42.93	72.69	-0.419
AVESA.00010b.r2.4DG0759170.1	AsADF13	142	15754.6	4.44	38.69	87.18	-0.238
AVESA.00010b.r2.4DG0759210.1	AsADF14	147	15837.76	4.6	39.09	85.65	-0.037
AVESA.00010b.r2.4DG0759220.1	AsADF15	142	16085.11	5.46	44.95	74.23	-0.487
AVESA.00010b.r2.5AG0799410.1	AsADF16	143	16402.91	8.73	43.25	74.34	-0.3
AVESA.00010b.r2.6AG1032230.1	AsADF17	139	16013.33	5.56	47.73	70.79	-0.384
AVESA.00010b.r2.7CG0705670.1	AsADF18	145	16746	5.94	43.45	74.69	-0.424

Chromosomal location and collinearity analysis of *AsADFs*

A total of 18 *AsADFs* were identified and distributed across 12 of the 20 chromosomes, with one to four genes per chromosome (Fig. 1). Chromosome 4D contained the highest number (*AsADF12*, *13*, *14,* and *15*), followed by chromosome 4A (*AsADF8*, *9,* and *10*), and chromosome 1D (*AsADF2* and *3*). The remaining chromosomes (1A, 2A, 2C, 2D, 3D, 4C, 5A, 6A, and 7C) each contained only one *AsADF* gene (Fig. 1).

Gene duplication is a widespread phenomenon that plays a crucial role in plant evolution [37]. To identify gene duplication events within the *AsADF* family, genomic collinearity segments in the oat genome were systematically analyzed using TBtools, and the results were visualized in Circos plots (Fig. 2). The results showed 13 pairs of tandem duplication events in the oat genome (Fig. 2). They suggest an evolutionary relationship between these *AsADF* members, and that these genes may have similar functions.

To further investigate the phylogenetic relationships between the oat *ADF* family and the *ADF* families of other plants, a collinearity analysis was conducted between oat and four other species: *A. thaliana,* maize,

rice, and wheat. The analysis revealed 3, 28, 17, and 44 orthologous gene pairs between oat and *A. thaliana*, maize, rice, and wheat, respectively. Notably, the *ADF* genes exhibited the highest degree of evolutionary conservation between oat and wheat (Fig. 3).

Phylogenetic analysis of the AsADFs

To further elucidate the phylogenetic relationships of oat ADF proteins, we collected *ADF* family genes from several identified species, including the model plant *A. thaliana*; the Poaceae species rice, maize, and wheat; and soybean (previously reported by our lab), and constructed a phylogenetic tree using the neighbor-joining (NJ) method in MEGA X with the ADF family of oat (Table S2, Fig. 4). The results showed that the ADF proteins were grouped into four groups, and the number in each group was different. With the exception of Group B, which contained only four Poaceae ADFs, the other three groups comprised ADFs from all six species. Notably, AsADFs and OsADFs within each subgroup showed a close evolutionary relationship. Among the oat ADFs, Group C contained the smallest number (3), while Groups A, B, and D each contained 4 members (Fig. 4).

Characteristics of the AsADFs protein sequences

The protein sequence identity among the AsADFs was greater than 58%, with the lowest identity observed between AsADF3 and AsADF14. Notably, the protein sequences of AsADF2/11/16 and AsADF8/18 were identical (Fig. S2). Multiple sequence alignment revealed that all AsADF proteins contain the conserved ADF-H domain and actin-binding regions (Fig. S3). Based on amino acid sequence prediction, the secondary structure of AsADF proteins consists mainly of three α-helices, six β-sheets, and four β-turns. This structural composition suggests that AsADF family proteins possess actin-binding functions, which is consistent with the known role of ADFs in binding to F-actin (Fig. S3). Furthermore, 3D structural models of AsADFs predicted by SWISS-MODEL show that proteins within the same group share high structural similarity, implying potential functional conservation (Fig. S4).

Conserved motifs and gene structures of the *AsADFs*

Among the nine conserved motifs identified, Motifs 1-4 constitute the core ADF domain, indicating their conservation and functional importance within the oat *ADF* family (Fig. 5B; Fig. S5). Notably, several motifs exhibited specific distributions: Motif 9 was unique to *AsADF1*; Motif 8 was exclusively present in *AsADF9* and *AsADF14*; Motif 6 was specific to Group C; and Motifs 5 and 7 were found only in Group D (Fig. 5B).

Structural analysis of *AsADF* genes revealed that members of the same group generally share similar exon-intron organizations (Fig. 5A, C). Within the *AsADF* gene family, all genes contained three exons, except for *AsADF4* and certain members of Group B (excluding *AsADF10*) (Fig. 5C). In these three exon genes, the second exon is the longest, flanked by shorter exons at the 5' and 3' ends, with the 3' exon being the shortest (Fig. 5C). Furthermore, size variation among the *AsADF* genes appears to be primarily due to differences in intron length.

Functional analysis of cis-elements in the promoter region of *AsADFs*

To further understand the functional roles of the *AsADF* gene family, we performed an analysis of the 2,000 bp promoter regions using the online software PlantCARE. The results showed that the cis-elements in the *AsADF* promoters could be classified into four major categories based on their predicted functions: stress response, photoperiod responsiveness, phytohormone response, and growth/development (Fig. 6; Fig. S6). Notably, the promoters of the *AsADF* family genes contained 11 low-temperature response and 21 drought responsive elements, suggesting their important roles in environmental stress adaptation. Furthermore, we identified 23 photoperiod-related and 9 hormone-related elements, with abscisic acid (ABA) and methyl jasmonate (MeJA) response elements being the most abundant (Fig. 6; Fig. S6). These findings suggest that the *AsADF* family is crucial not only for growth and development but also for responding to abiotic stresses in oat.

Analysis of differential expression under circadian rhythm

To further investigate the potential roles of *AsADF* genes in oat growth, we analyzed their circadian expression rhythms by qRT-PCR. In all qRT-PCR analyses, a gene was considered to respond to a treatment if it showed a minimum twofold difference compared to the control with a statistical significance of $P < 0.01$. The results showed that *AsADF* genes in the same group had similar rhythmic expression patterns (Fig. 7). Specifically, in Group A, the expression levels of four genes (excluding *AsADF17*) exhibited a circadian rhythm, being up-regulated after sunrise (8:00), peaking at noon (12:00), and subsequently down-regulated. Conversely, Group C genes displayed an opposite pattern, with the highest expression at 8:00 that decreased throughout the day and began to rise again around 24:00. Within Group D, *AsADF8*, *12*, and *18* showed the same expression pattern as Group C, with levels down-regulated during the day and up-regulated at night to a peak at 24:00, but *AsADF1*, *AsADF3* and all Group B genes did not exhibit significant circadian rhythmicity (Fig. 7). In summary, the expression of most *AsADF* genes exhibits diurnal fluctuations, suggesting their involvement in photoperiod-related growth and development processes.

Transcription patterns of *AsADFs* in response to abiotic stress

To further understand the potential functions of *AsADFs* in response to abiotic stresses, we collected leaves and roots from oat seedlings at the three-leaf stage following exposure to cold, heat, drought, and salt treatments. The relative expression levels of the *AsADF* genes were then examined by qRT-PCR (Fig. 8). The results indicated that most *AsADF* genes were responsive to various abiotic stresses to differing degrees. Notably, the expression of *AsADF4*, *5* and *7* of Group A, *AsADF9*, *13*, and *14* of Group B, *AsADF8*, *12* and *18* of Group D responded to all four stress treatments, suggesting their potential essential functions in oat's stress response. The expression levels of *AsADF9*, *13* and *14* were significantly up-regulated under all four stresses; those of *AsADF8*, *12* and *18* were up-regulated by heat, salt, and drought stress, while under cold stress, their expression was initially up-regulated, peaked at 3 h and subsequently down-regulated; The relative expression of *AsADF4*, *5*, and *7* was down-regulated under heat and salt stress, but under cold stress, their expression was initially down-regulated, up-regulated at 12 h, and then down-regulated again, drought stress caused little overall change, although a transient spike in expression was notably observed at 9 h. Under cold stress treatment, the expression levels of the 13 *AsADF* genes, except for *AsADF1*, *3*, *10*, *15*, and *17*, were up-regulated or down-regulated to varying degrees; whereas under drought stress, the expression levels of all

AsADF genes were up-regulated, among which the expression levels of *AsADF9*, *13* and *14* were up-regulated by more than a 100-fold (Fig. 8).

Discussion

ADFs, recognized as one of the key members among ABPs, are involved in many plant growth and development processes [5, 9]. Their crucial role in plant stress responses has been well-established [5]. The *ADF* gene family has been identified in a variety of plant species through genome-wide analyses. The number of *ADF* genes varies, with 11 in *A. thaliana*, 11 in rice, 14 in poplar, 11 in tomato, 27 in banana, 13 in maize, 9 in common bean, 10 in pigeon pea, 25 in wheat, 18 in soybean, 18 in melon, 18 in Chinese cabbage, and 9 in alfalfa [11, 22, 26, 38–47]. However, the functions of the *ADF* family genes in oats remain unclear. Therefore, we identified *ADF* genes in oat and conducted a comprehensive analysis of their phylogenetic relationships, sequence characteristics, and expression patterns.

In this study, we identified 18 *ADF* genes (Fig. 1, Table 1), which were located on 12 chromosomes (Fig. 1). Previous studies have suggested that *ADF* genes in plants likely evolved from a common ancestor [41]. A comparative analysis of the characterized *ADF* families in Poaceae reveals that this number of ADF genes is greater than that in rice (11) and maize (13) but less than that in wheat (25). This variation in gene copy number among different plant species is potentially driven by gene duplication events [11, 22, 26, 48]. Although oats and wheat are both important allopolyploid cereals with complex and large genomes, we found that oats possess a smaller number of *ADF* genes than wheat [26]. We speculate that this difference from the relatively late initiation of systematic research on oats compared to wheat, resulting in a less complete genome assembly and annotation.

Evolutionary analysis indicated that oat *ADF* genes were classified into four groups (Fig. 4). This grouping pattern is consistent with that reported in *A. thaliana*, rice, tomato, maize, melon, soybean, Chinese cabbage, and alfalfa [11, 38, 40, 44–47]. Phylogenetic analysis revealed that many oat *ADF* genes were closely clustered with previously reported *ADF* genes known to play critical roles in stress responses, suggesting potential functional conservation. For instance, *AsADF9*, *AsADF13*, and *AsADF14* cluster within the same clade as *OsADF3* and *TaADF16*. Based on the reported roles of these genes in drought and cold stress tolerance, we speculate that the oat *ADFs* in this clade may exhibit a conserved biological function in response to these abiotic stresses [22, 26](Fig. 4). Furthermore, the exon-intron structures of these genes were largely conserved compared to previous reports (Fig. 5C). Analysis of the oat ADF protein motifs revealed that these proteins are highly conserved (Fig. 5B). All AsADF proteins contain the ADF-H domain, which is composed of motifs 1 to 4. Additionally, we identified some motifs specific to certain genes, which may be linked to functional specialization among them (Fig. 5B; Fig. S5).

Given that gene expression is largely regulated by cis-elements in promoter sequences, analyzing these elements helps elucidate the regulatory mechanisms of *ADF* genes and infer their potential biological functions [49, 50]. Previous studies have indicated that phytohormonal signals and environmental stresses are key regulators of *ADF* gene expression [17, 26]. Various phytohormone and stress-responsive elements, including LTR (low-temperature response), MBS (drought stress response), ABRE (ABA response), and TGACG-/CGTAC-motifs (MeJA response), were identified in the promoters of oat *ADF* genes through cis-

element analysis (Fig. 6; Fig. S6). Notably, light-responsive elements were also identified in all *AsADF* gene promoters, further supporting their potential roles in regulating oat growth, development, and stress responses.

Light is fundamental to plant life, and its perception governs key aspects of plant growth and development [51–53]. The expression of numerous genes involved in these processes is under circadian rhythm regulation, which in turn affects the growth and development of plants [54]. Given the presence of multiple light-responsive elements identified in the promoters of oat *ADF* genes, we speculate that they might function in photoperiodic regulation (Fig. 6; Fig. S6). To investigate whether there was differential circadian expression of the *AsADF* genes, we conducted qRT-PCR analysis (Fig. 7). Our results indicated that the expression of most *AsADF* genes followed a circadian rhythm (Fig. 7). Genes in Group A (except *AsADF17*) exhibited higher expression during the day than at night, with their transcript levels peaking at noon coinciding with the highest temperature of the day, suggesting a potential role in sensing ambient temperature fluctuations. Conversely, the Group C genes showed higher expression during the night. Phylogenetic relationships showed these genes are in the same clade as *AtADF5*, which has been reported to regulate drought tolerance by modulating stomatal aperture. Based on this, we infer that the Group C *AsADFs* may perform a similar function in drought stress response [18](Fig. 4; Fig. 7). In summary, *AsADF* genes likely participate in various growth and developmental pathways by responding to photoperiodic rhythms.

During growth and development, plants are usually exposed to various environmental stresses, such as soil salinity, drought, and extreme temperatures [55]. As an important nutrient-rich grain and forage crop, oat holds significant value in stable yields under stress conditions [27–29]. Plants require optimal temperatures for growth and development, and temperatures beyond their physiological optimum ranges can result in heat or cold stress [56]. With the intensification of global warming in recent years, the fluctuations in spring temperatures have significantly increased the risk of cereal crops being exposed to late spring coldness (LSC) [57, 58]. LSC causes severe damage or even plant death. As oats are mainly cultivated in cold high-altitude regions, they are highly vulnerable to LSC, often leading to significant yield losses. Moreover, oat growth requires cool climatic conditions, and this trait limits its cultivation in warmer regions and constrains the supply of high-quality oats to meet consumer demand [59, 60]. Besides temperature stress, salt and drought stress also negatively affect oat growth and productivity [61, 62]. Soil salinization is a major environmental challenge to global agricultural production [34, 63], and drought conditions are common in many oat-growing regions. Although oats are moderately stress tolerant, their yield remains limited by salt and drought [34, 35, 64]. Therefore, identifying key genes associated with abiotic stress tolerance is crucial for oat's stable yields. The remodeling of the actin cytoskeleton serves as a critical target for signaling pathways triggered by diverse developmental and environmental stimuli [8, 65]. Plant *ADFs* function through cytoskeletal remodeling, and studies have reported that *ADF* genes in various Poaceae species participate in abiotic stress responses. For instance, heterologous expression of *OsADF3* enhances drought tolerance in *A. thaliana* [22]. In addition, *TaADF16* plays an important role in low temperature tolerance [26]. Based on the significant role of the *ADF* gene family in abiotic stress responses, it is necessary to analyze its function in oats. Leaves are the primary site for temperature stress perception in plants, while roots are a major organ for sensing salt and drought stress. Therefore, we used qRT-PCR to analyze the expression patterns of *AsADF* genes under these stresses [66, 67]. As shown in Fig. 8, all *AsADF* genes were responsive to drought stress.

Notably, Group B members *AsADF9*, *AsADF13*, and *AsADF14* exhibited significant up-regulation under all four abiotic stress treatments, suggesting their important role in stress response of oats (Fig. 8). These *ADF* genes are potential candidates for abiotic stress tolerance in oats and could be further verified as key genes.

Conclusions

This study identified 18 *ADF* genes unevenly distributed across 12 chromosomes in the oat genome. Phylogenetic analysis classified these genes into four groups, with members of each group exhibiting conserved gene structures and motif compositions. Expression analysis revealed that most *ADF* genes showed circadian rhythms, suggesting roles in plant growth regulation. Furthermore, multiple *ADF* genes responded to various abiotic stresses, particularly drought, indicating their potential involvement in stress adaptation. Notably, *AsADF9*, *AsADF13*, and *AsADF14* from Group B were significantly up-regulated under four stress conditions, indicating that they are promising candidates for further functional characterization. These results provide valuable insights into the functions of the *ADF* family and offer new genetic resources for the development of stress-tolerant oat varieties.

Materials and methods

Identification of the ADF genes in the genome of oat

The whole genome and GFF3 of oat (Sang.v1.1) and other plants (*A. thaliana*, rice, maize, and wheat) were obtained from the Ensembl Plants database (https://plants.ensembl.org/).

A collection of experimentally validated *ADF* family sequences from published studies served as query sequences for homology-based screening via the BLAST Compare Two Seqs function in TBtools [68]. The hidden Markov model (HMM) profile of the ADF-H domain (PF00241) was obtained from the Pfam database (http://pfam.xfam.org/) and domain architecture analysis was conducted using the Simple HMM Search module within TBtools with an E-value cutoff of 1e-5.

The presence of the ADF-H domain in putative ADF proteins was verified using the batch CD-search tool available through the NCBI Conserved Domain Database (CDD) (https://www.ncbi.nlm.nih.gov/Structure/bwrpsb/bwrpsb.cgi).

A consensus strategy integrating sequence similarity and structural domain conservation yielded the final candidate set of oat *ADF* family members.

Physicochemical characteristics and localization to chromosomes

The physicochemical properties of the identified AsADF proteins, including amino acid length, molecular weight (MW), isoelectric point (pI), instability index (II), aliphatic index (AI), and grand average of hydropathicity (GRAVY), were predicted using the ProtParam tool on the ExPASy server [69] (https://web.expasy.org/protparam/).

The physical positions of the *AsADF* genes were determined from the genome annotation file, and the genes were mapped to their chromosomes. The genomic distribution was visualized using the "Gene Location Visualize from GTF/GFF" function in TBtools, based on the Sang reference genome.

Analysis of the gene structure and identification of the conserved motif in the protein

Structural analysis of *AsADF* genes was performed using the oat genome annotation file (GFF3 format) obtained from the Ensembl Plants database. A phylogenetic tree of AsADF proteins was constructed with MEGA X software via the NJ method, with 1000 bootstrap replicates. Conserved motifs in the AsADF proteins were identified using the MEME (Multiple Expectation Maximization for Motif Elicitation) suite, with the maximum number of motifs set to 9, and were visualized using the "Gene Structure View" function in TBtools. Exon-intron structures were visualized using the "Visualize Gene Structure" function in TBtools. Furthermore, conserved domains in AsADF proteins were predicted using the Batch CD-Search tool on the NCBI platform and visualized with the "Visualize NCBI CDD Domain Pattern" function in TBtools.

Analysis of protein sequence characteristics, phylogeny, and collinearity

Multiple sequence alignment of ADF family proteins was performed using MEGA X software, and the resulting alignment was exported in FASTA format. For visualization, the tertiary structure file of the ADF protein (1f7s.1.pdb) was obtained from SWISS-MODEL and used to annotate the alignment results using the online tool ESPript 3.0. The protein sequences of the 18 *AsADF* genes were submitted to the SWISS-MODEL online server [70] (https://swissmodel.expasy.org/) for homology modeling. The template (1f7s.1.A) with the highest Global Model Quality Estimation (GMQE) score in the PDB database was selected to ensure high structural consistency across the AsADF protein family.The phylogenetic tree of oat, wheat, rice, and maize ADF proteins was constructed using the NJ method in MEGA X software with 1000 bootstrap replicates. The resulting tree was then visualized and annotated using the iTOL online platform (https://itol.embl.de/) to enhanced graphical representation.

Gene collinearity analysis was carried out among *A. thaliana*, wheat, rice, and maize. The One-Step MCScanX-Super Fast plugin in TBtools was employed for the collinearity analysis and visualization.

Cis-elements analysis and subcellular localization

Putative cis-acting elements within the 2,000 bp promoter region upstream of the *AsADF* genes were identified using the PlantCARE database (https://bioinformatics.psb.ugent.be/webtools/plantcare/html/). The predicted cis-acting elements were visualized using TBtools.

Subcellular localization was predicted using WoLF PSORT (https://wolfpsort.hgc.jp/). The results were subsequently visualized and comparatively analyzed with TBtools to facilitate biological interpretation.

Plant materials and stress treatments materials of oat seedlings

The oat cultivar Keyan No.4, used in this study, was developed and stored at the Key Laboratory of Adaptation and Evolution of Plateau Biota (AEPB) of the Northwest Institute of Plateau Biology, Chinese Academy of Sciences. The oat seeds were disinfected using 75% ethanol for 5 min, followed by treatment with 3% H_2O_2 for 1 min, and then washed 5 times with sterile water before being germinated for 5 days in a growth chamber.

The germinated seeds were then cultivated in a modified Hoagland solution (NS10205-500 mL, Coolaber) under a 14-h light/10-h dark cycle, with temperatures at 23°C during the day and 18°C at night for 15 days. Subsequently, seedlings were exposed to various stress conditions: heat (40°C), cold (4°C), salt (150 mM NaCl), and drought (simulated with 20% w/v PEG-6000), for durations of 0, 1, 3, 6, 12, and 24 hours. Untreated Hoagland's solution was used as the control. For circadian rhythm analysis of *AsADFs*, seedlings were grown until the three-leaf stage, and samples were collected every 4 hours. Following collection, roots and leaves were immediately frozen in liquid nitrogen and stored at -80°C for subsequent RNA extraction.

RNA extraction, cDNA preparation, and quantitative real-time PCR (qRT-PCR)

Total RNA was extracted from plant samples using FastPure Universal Plant Total RNA Isolation Kit (RC411-01, Vazyme) according to the manufacturer's instructions. And then reverse-transcribed into cDNA with HiScriptIII RT SuperMix for qPCR (+ gDNA wiper) (R323-01, Vazyme). The qRT-PCR analysis was performed using ChamQ Universal SYBR qPCR Master Mix (Q711, Vazyme Biotech), and the protocol was 95℃ for 30 s followed by 34 cycles of 95 ℃ for 10 s and 60 ℃ for 30 s. Relative quantification of gene expression was performed based on the $2^{-\Delta\Delta Ct}$ method [71], with *AsEIF4A* used as the internal reference gene. The sequences of all primers used in this study are listed in Supplementary Table S3.

Data analysis

Data were analyzed using SPSS 22 (SPSS Inc., USA) and GraphPad Prism 8 (GraphPad Software Inc., USA). Continuous variables are expressed as mean ± standard deviation (SD). Differences between the control and treatment groups at various time points were evaluated using t-tests. For comparisons among multiple treatment conditions, one-way ANOVA was applied. A p-value of less than 0.05 was considered statistically significant.

Declarations

Ethics approval and consent to participate

Not applicable.

Consent for publication

Not applicable.

Competing interests

The authors declare no competing interests.

Funding

This work was supported by National Major Agricultural Science and Technology Project (NK20220402), National Natural Science Foundation of China (U24A20427), and the Qinghai Provincial Key Laboratory of Crop Molecular Breeding (2023-1-1).

Author Contribution

D.W. and T.L. conceived and designed the research. H.C. and B.Z. guided the experiment. D.W. and G.W. conducted the experiments. D.W. and B.Z. wrote the manuscript. W.T. H.C. and G.W. provided technical assistance. T.L. and W.T. critically reviewed and revised the manuscript. All authors have read and agreed to the published version of the manuscript.

Acknowledgements

Not applicable.

Data Availability

The genome sequences and annotation files of oat, *A. thaliana* , maize, rice, and wheat were downloaded from the Ensembl Plants database (https://plants.ensembl.org/index.html).

References

1. Bamburg JR, McGough A, Ono S. Putting a new twist on actin: ADF/cofilins modulate actin dynamics. Trends Cell Biol. 1999;9(9):364–70.
2. Pollard TD, Cooper JA. Actin, a central player in cell shape and movement. Science. 2009;326(5957):1208–12.
3. Porter K, Day B. From filaments to function: The role of the plant actin cytoskeleton in pathogen perception, signaling and immunity. J Integr Plant Biol. 2016;58(4):299–311.
4. Dominguez R, Holmes KC. Actin structure and function. Annu Rev Biophys. 2011;40:169–86.
5. Sun Y, Shi M, Wang D, Gong Y, Sha Q, Lv P, et al. Research progress on the roles of actin-depolymerizing factor in plant stress responses. Front Plant Sci. 2023;14:1278311.
6. Kristó I, Bajusz I, Bajusz C, Borkúti P, Vilmos P. Actin, actin-binding proteins, and actin-related proteins in the nucleus. Histochem Cell Biol. 2016;145(4):373–88.
7. Higaki T, Sano T, Hasezawa S. Actin microfilament dynamics and actin side-binding proteins in plants. Curr Opin Plant Biol. 2007;10(6):549–56.
8. Ma Z, Miao Y. Review: F-Actin remodelling during plant signal transduction via biomolecular assembly. Plant Sci. 2020;301:110663.

9. Inada N. Plant actin depolymerizing factor: actin microfilament disassembly and more. J Plant Res. 2017;130(2):227–38.
10. Hussey PJ, Allwood EG, Smertenko AP. Actin-binding proteins in the *Arabidopsis* genome database: properties of functionally distinct plant actin-depolymerizing factors/cofilins. Philos Trans R Soc Lond B Biol Sci. 2002;357(1422):791–8.
11. Huang J, Sun W, Ren J, Yang R, Fan J, Li Y, et al. Genome-wide identification and characterization of actin-depolymerizing factor (ADF) family genes and expression analysis of responses to various stresses in *Zea Mays* L. Int J Mol Sci. 2020;21(5).
12. Burgos-Rivera B, Ruzicka DR, Deal RB, McKinney EC, King-Reid L, Meagher RB. ACTIN DEPOLYMERIZING FACTOR9 controls development and gene expression in *Arabidopsis*. Plant Mol Biol. 2008;68(6):619–32.
13. Zhao S, Zhao Y, Guo Y. 14-3-3 λ protein interacts with ADF1 to regulate actin cytoskeleton dynamics in *Arabidopsis*. Sci China Life Sci. 2015;58(11):1142–50.
14. Yao H, Li X, Peng L, Hua X, Zhang Q, Li K, et al. Binding of 14-3-3κ to ADF4 is involved in the regulation of hypocotyl growth and response to osmotic stress in *Arabidopsis*. Plant Sci. 2022;320:111261.
15. Wang J, Shen J, Xu Y, Jiang Y, Qu X, Zhao W, et al. Differential sensitivity of ADF isovariants to a pH gradient promotes pollen tube growth. J Cell Biol. 2023;222(11).
16. Wang HY, Wang J, Gao P, Jiao GL, Zhao PM, Li Y, et al. Down-regulation of *GhADF1* gene expression affects cotton fibre properties. Plant Biotechnol J. 2009;7(1):13–23.
17. Lv G, Li Y, Wu Z, Zhang Y, Li X, Wang T, et al. Maize actin depolymerizing factor 1 (*ZmADF1*) negatively regulates pollen development. Biochem Biophys Res Commun. 2024;703:149637.
18. Qian D, Zhang Z, He J, Zhang P, Ou X, Li T, et al. *Arabidopsis ADF5* promotes stomatal closure by regulating actin cytoskeleton remodeling in response to ABA and drought stress. J Exp Bot. 2019;70(2):435–46.
19. Wang L, Qiu T, Yue J, Guo N, He Y, Han X, et al. *Arabidopsis ADF1* is regulated by MYB73 and is involved in response to salt stress affecting actin filament organization. Plant Cell Physiol. 2021;62(9):1387–95.
20. Sun Y, Zhong M, Li Y, Zhang R, Su L, Xia G, et al. *GhADF6*-mediated actin reorganization is associated with defence against *Verticillium dahliae* infection in cotton. Mol Plant Pathol. 2021;22(12):1656–67.
21. Wang D, Du M, Lyu P, Li J, Meng H, Liu X, et al. Functional characterization of the soybean *glycine max* actin depolymerization factor *GmADF13* for plant resistance to drought stress. Plants (Basel). 2024;13(12).
22. Huang YC, Huang WL, Hong CY, Lur HS, Chang MC. Comprehensive analysis of differentially expressed rice actin depolymerizing factor gene family and heterologous overexpression of *OsADF3* confers *Arabidopsis thaliana* drought tolerance. Rice (N Y). 2012;5(1):33.
23. Tang C, Deng L, Chang D, Chen S, Wang X, Kang Z. TaADF3, an actin-depolymerizing factor, negatively modulates wheat resistance against *Puccinia striiformis*. Front Plant Sci. 2015;6:1214.
24. Fu Y, Duan X, Tang C, Li X, Voegele RT, Wang X, et al. TaADF7, an actin-depolymerizing factor, contributes to wheat resistance against *Puccinia striiformis* f. sp. tritici. Plant J. 2014;78(1):16–30.
25. Zhang B, Hua Y, Wang J, Huo Y, Shimono M, Day B, et al. TaADF4, an actin-depolymerizing factor from wheat, is required for resistance to the stripe rust pathogen *Puccinia striiformis* f. sp. tritici. Plant J.

2017;89(6):1210–24.
26. Xu K, Zhao Y, Zhao S, Liu H, Wang W, Zhang S, et al. Genome-wide identification and low temperature responsive pattern of actin depolymerizing factor (ADF) gene family in wheat (*Triticum aestivum* L.). Front Plant Sci. 2021;12:618984.
27. Menon R, Gonzalez T, Ferruzzi M, Jackson E, Winderl D, Watson J. Oats-from farm to fork. Adv Food Nutr Res. 2016;77:1–55.
28. Singh S, Koli P, Ahmed S, Kumar N, Rana M, Singhal R, et al. Exploring the genetic variability in yield, nutritional and digestibility traits in oat grains through ruminant nutrition. Heliyon. 2024;10(10):e31541.
29. Duan H, Liu L, Wang W, Li S, Shi Z, Liang G, et al. Stay-green trait enhances grain yield, nutritional quality, and seed germination ability in oat (*Avena sativa* L.) on the Qinghai-tibet plateau. Plants (Basel). 2025;14(16).
30. Sirotkin AV. The Effect of Dietary oat consumption and its constituents on fat storage and obesity. Physiol Res. 2023;72(Suppl 2):S157–s63.
31. Kundi ZM, Lee JC, Pihlajamäki J, Chan CB, Leung KS, So SSY, et al. Dietary fiber from oat and rye brans ameliorate western diet-induced body weight gain and hepatic inflammation by the modulation of short-chain fatty acids, bile acids, and tryptophan metabolism. Mol Nutr Food Res. 2021;65(1):e1900580.
32. Akbari Moghaddam Kakhki R, Navarro-Villa A, de Los Mozos J, de Vries S, García-Ruiz AI. Evaluation of fibrous feed ingredients alternatives to oat hulls as a source of feed structure in broiler diets. Poult Sci. 2024;103(12):104297.
33. Hanoğlu Oral H. Forage yields and nutritive values of oat and triticale pastures for grazing sheep in early spring. PeerJ. 2024;12:e17840.
34. Zhang MX, Bai R, Nan M, Ren W, Wang CM, Shabala S, et al. Evaluation of salt tolerance of oat cultivars and the mechanism of adaptation to salinity. J Plant Physiol. 2022;273:153708.
35. Wen G, Ma BL, Shi Y, Liu K, Chen W. Selection of oat (*Avena sativa* L.) drought-tolerant genotypes based on multiple yield-associated traits. J Sci Food Agric. 2023;103(9):4380–91.
36. Lee JS, Ko CS, Seo YW. Oat AsDA1-2D enhances heat stress tolerance and negatively regulates seed-storage globulin. J Plant Physiol. 2023;284:153981.
37. Rensing SA. Gene duplication as a driver of plant morphogenetic evolution. Curr Opin Plant Biol. 2014;17:43–8.
38. Feng Y, Liu Q, Xue Q. Comparative study of rice and *Arabidopsis* actin-depolymerizing factors gene families. J Plant Physiol. 2006;163(1):69–79.
39. Roy-Zokan EM, Dyer KA, Meagher RB. Phylogenetic patterns of codon evolution in the ACTIN-DEPOLYMERIZING FACTOR/COFILIN (ADF/CFL) gene family. PLoS One. 2015;10(12):e0145917.
40. Khatun K, Robin AH, Park JI, Kim CK, Lim KB, Kim MB, et al. Genome-wide identification, characterization and expression profiling of *ADF* Family Genes in *Solanum lycopersicum* L. Genes (Basel). 2016;7(10).
41. Nan Q, Qian D, Niu Y, He Y, Tong S, Niu Z, et al. Plant actin-depolymerizing factors possess opposing biochemical properties arising from key amino acid changes throughout evolution. Plant Cell. 2017;29(2):395–408.

42. Ortega-Ortega Y, Carrasco-Castilla J, Juárez-Verdayes MA, Toscano-Morales R, Fonseca-García C, Nava N, et al. Actin depolymerizing factor modulates rhizobial infection and nodule organogenesis in common bean. Int J Mol Sci. 2020;21(6).
43. Cao H, Amin R, Niu L, Song Z, Dong B, Li H, et al. Multidimensional analysis of actin depolymerising factor family in pigeon pea under different environmental stress revealed specific response genes in each subgroup. Funct Plant Biol. 2021;48(2):180–94.
44. Sun Y, Wang D, Shi M, Gong Y, Yin S, Jiao Y, et al. Genome-wide identification of actin-depolymerizing factor gene family and their expression patterns under various abiotic stresses in soybean (*Glycine max*). Front Plant Sci. 2023;14:1236175.
45. Lv Y, Liu S, Zhang J, Cheng J, Wang J, Wang L, et al. Genome-wide identification of actin-depolymerizing factor family genes in melon (*Cucumis melo* L.) and *CmADF1* plays an important role in low temperature tolerance. Front Plant Sci. 2024;15:1419719.
46. Wang W, Qu G, Sun Y, Chen J, Feng H, Gao Y. Genome-wide identification of *ADF* gene family in Chinese cabbage (*Brassica rapa* L. ssp. pekinensis) and functional characterization of *BrADF11* under heat stress. Plant Physiol Biochem. 2025;223:109796.
47. Shi M, Wang Y, Lv P, Gong Y, Sha Q, Zhao X, et al. Genome-wide characterization and expression analysis of the *ADF* gene family in response to salt and drought stress in alfalfa (*Medicago sativa*). Front Plant Sci. 2024;15:1520267.
48. Cannon SB, Mitra A, Baumgarten A, Young ND, May G. The roles of segmental and tandem gene duplication in the evolution of large gene families in *Arabidopsis thaliana*. BMC Plant Biol. 2004;4:10.
49. Narusaka Y, Nakashima K, Shinwari ZK, Sakuma Y, Furihata T, Abe H, et al. Interaction between two cis-acting elements, ABRE and DRE, in ABA-dependent expression of *Arabidopsis rd29A* gene in response to dehydration and high-salinity stresses. Plant J. 2003;34(2):137–48.
50. Priest HD, Filichkin SA, Mockler TC. Cis-regulatory elements in plant cell signaling. Curr Opin Plant Biol. 2009;12(5):643–9.
51. Jackson SD. Plant responses to photoperiod. New Phytol. 2009;181(3):517–31.
52. de Wit M, Galvão VC, Fankhauser C. Light-mediated hormonal regulation of plant growth and development. Annu Rev Plant Biol. 2016;67:513–37.
53. Li X, Liang T, Liu H. How plants coordinate their development in response to light and temperature signals. Plant Cell. 2022;34(3):955–66.
54. Izawa T. Physiological significance of the plant circadian clock in natural field conditions. Plant Cell Environ. 2012;35(10):1729–41.
55. Zhu JK. Abiotic stress signaling and responses in plants. Cell. 2016;167(2):313–24.
56. Huang J, Zhao X, Bürger M, Chory J, Wang X. The role of ethylene in plant temperature stress response. Trends Plant Sci. 2023;28(7):808–24.
57. Jiang G, Hassan MA, Muhammad N, Arshad M, Chen X, Xu Y, et al. Comparative physiology and transcriptome analysis of young spikes in response to late spring coldness in wheat (*Triticum aestivum* L.). Front Plant Sci. 2022;13:811884.

58. Fang H, Huang J, Zhu X, Hassan MA, Ren J, Huang J, et al. Postponed application of phosphorus and potassium fertilizers mitigates the damage of late spring coldness by improving winter wheat root physiology. Plants (Basel). 2024;13(16).
59. Qin M, Gao X, Feng M, Jin N, Wang C, Cheng W. Modeling of the potential geographical distribution of naked oat under climate change. Front Plant Sci. 2022;13:1009577.
60. Sun Y, Jing H, Li Z, Wan K, Ma J, Zhang H, et al. Integrated transcriptomic, metabolomic and lipidomic analyses uncover the crucial roles of lipid metabolism pathways in oat (*Avena sativa*) responses to heat stress. BMC Genomics. 2025;26(1):780.
61. Zhang JL, Shi H. Physiological and molecular mechanisms of plant salt tolerance. Photosynth Res. 2013;115(1):1–22.
62. Angon PB, Tahjib-Ul-Arif M, Samin SI, Habiba U, Hossain MA, Brestic M. How do plants respond to combined drought and salinity stress?-a systematic review. Plants (Basel). 2022;11(21).
63. Xu Z, Shao T, Lv Z, Yue Y, Liu A, Long X, et al. The mechanisms of improving coastal saline soils by planting rice. Sci Total Environ. 2020;703:135529.
64. Zhu G, Liu J, Wu H, Zhu Y, Nimir NEA, Zhou G. The optimum mixed cropping ratio of oat and alfalfa enhanced plant growth, forage yield, and forage quality in saline soil. Plants (Basel). 2024;13(21).
65. Lian N, Wang X, Jing Y, Lin J. Regulation of cytoskeleton-associated protein activities: Linking cellular signals to plant cytoskeletal function. J Integr Plant Biol. 2021;63(1):241–50.
66. Gupta A, Rico-Medina A, Caño-Delgado AI. The physiology of plant responses to drought. Science. 2020;368(6488):266–9.
67. Zoong Lwe Z, Sah S, Persaud L, Li J, Gao W, Raja Reddy K, et al. Alterations in the leaf lipidome of Brassica carinata under high-temperature stress. BMC Plant Biol. 2021;21(1):404.
68. Chen C, Chen H, Zhang Y, Thomas HR, Frank MH, He Y, et al. TBtools: an integrative toolkit developed for interactive analyses of big biological data. Mol Plant. 2020;13(8):1194–202.
69. Wilkins MR, Gasteiger E, Bairoch A, Sanchez JC, Williams KL, Appel RD, et al. Protein identification and analysis tools in the ExPASy server. Methods Mol Biol. 1999;112:531–52.
70. Waterhouse A, Bertoni M, Bienert S, Studer G, Tauriello G, Gumienny R, et al. SWISS-MODEL: homology modelling of protein structures and complexes. Nucleic Acids Res. 2018;46(W1):W296–w303.
71. Derveaux S, Vandesompele J, Hellemans J. How to do successful gene expression analysis using real-time PCR. Methods. 2010;50(4):227–30.

Figures

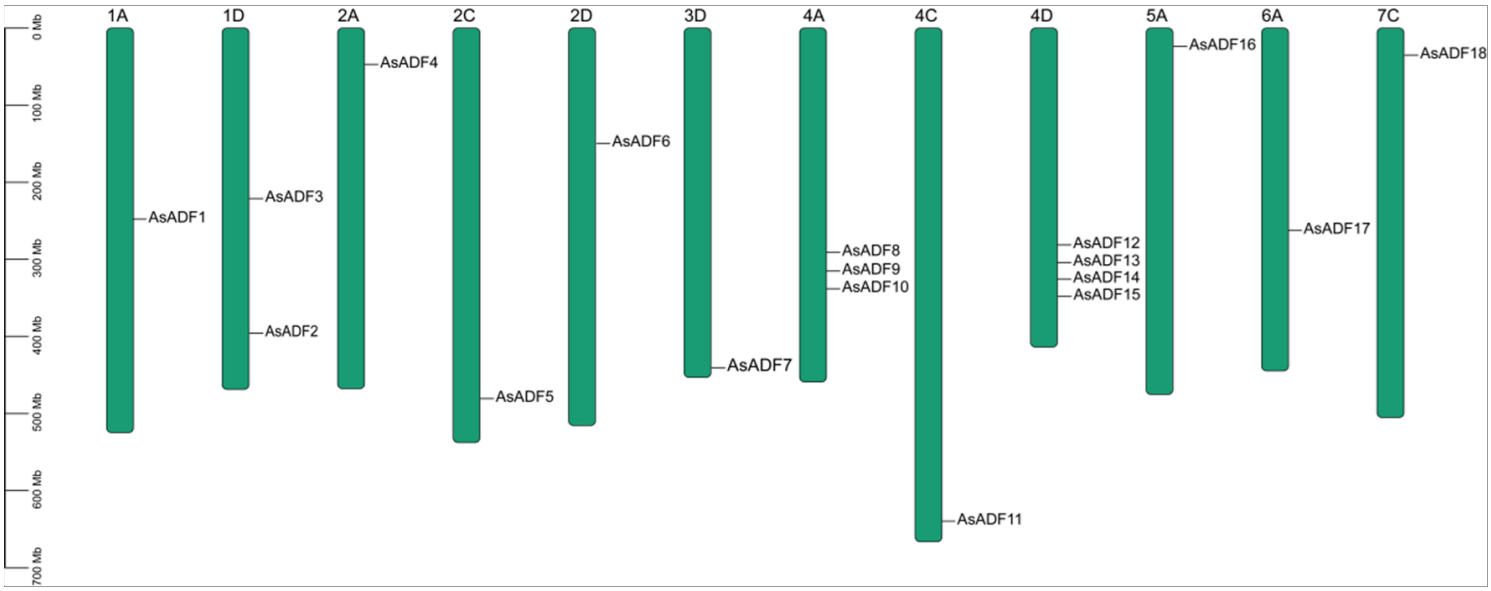

Figure 1

Chromosomal locations of the *ADF* gene family.

Green bars represent the twelve chromosomes with *AsADF* genes. The scale indicates the chromosome length, and the black lines indicate the position of each *AsADF* gene.

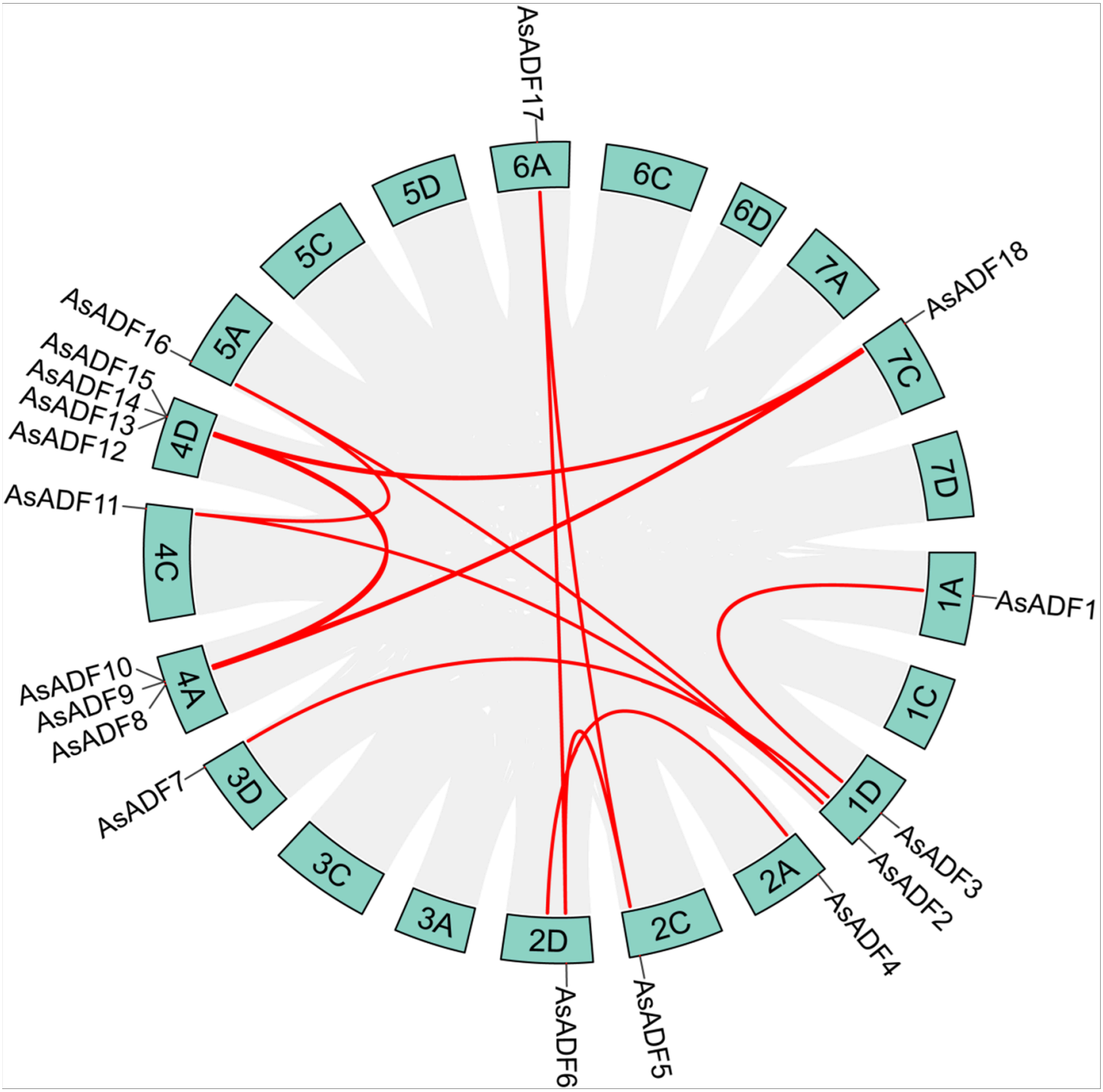

Figure 2

Chromosome localization of *AsADF* duplicated genes in oat.

The green boxes represent different chromosomes.

The red lines represent the segmentally duplicated genes.

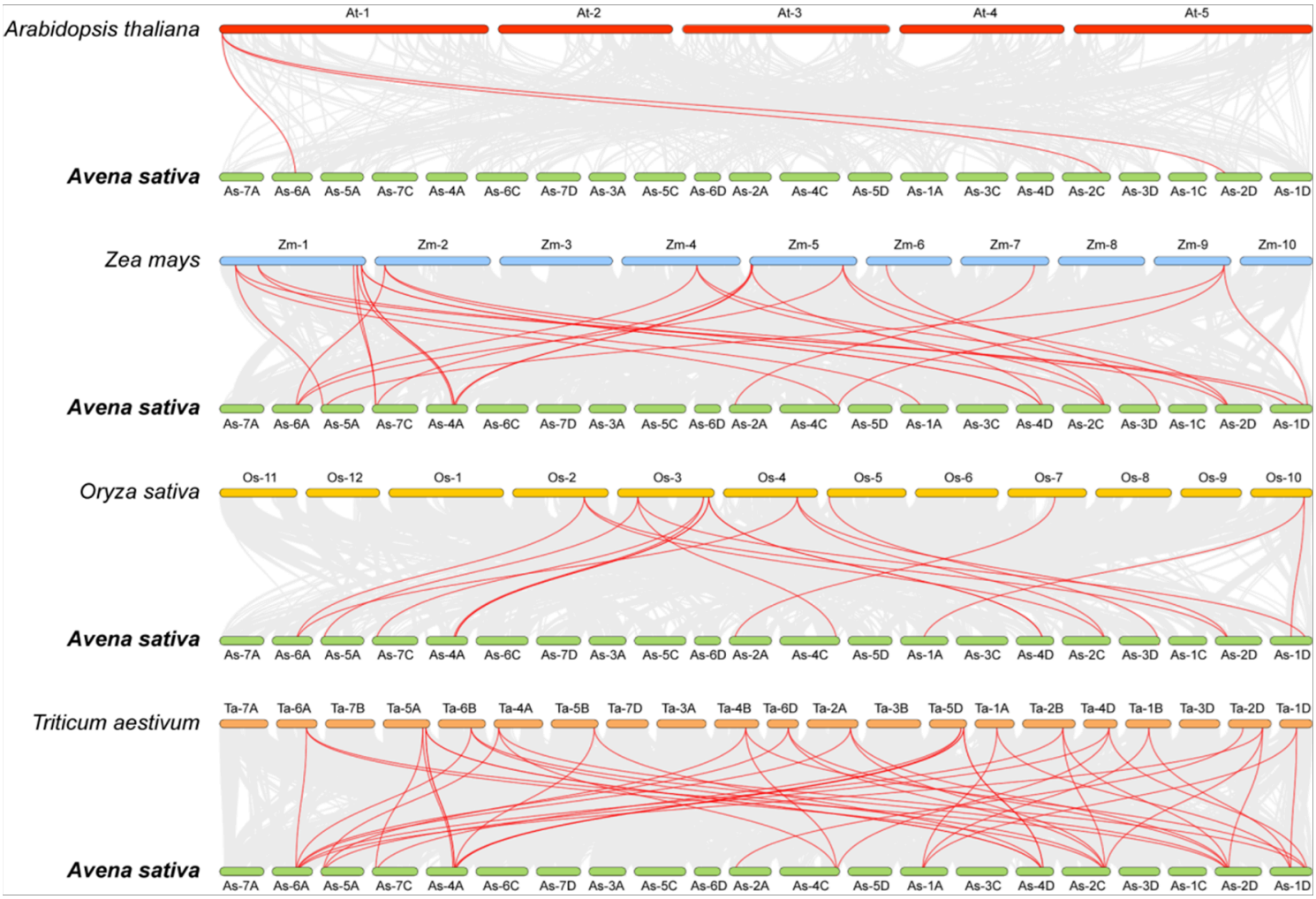

Figure 3

Synteny analyses of the *ADF* genes between oat and four representa-tive species.

The collinear blocks within *A. sativa* and other specie genomes were displayed by the gray lines.

The syntenic *ADF* gene pairs between oat and other species were highlighted with the red lines.

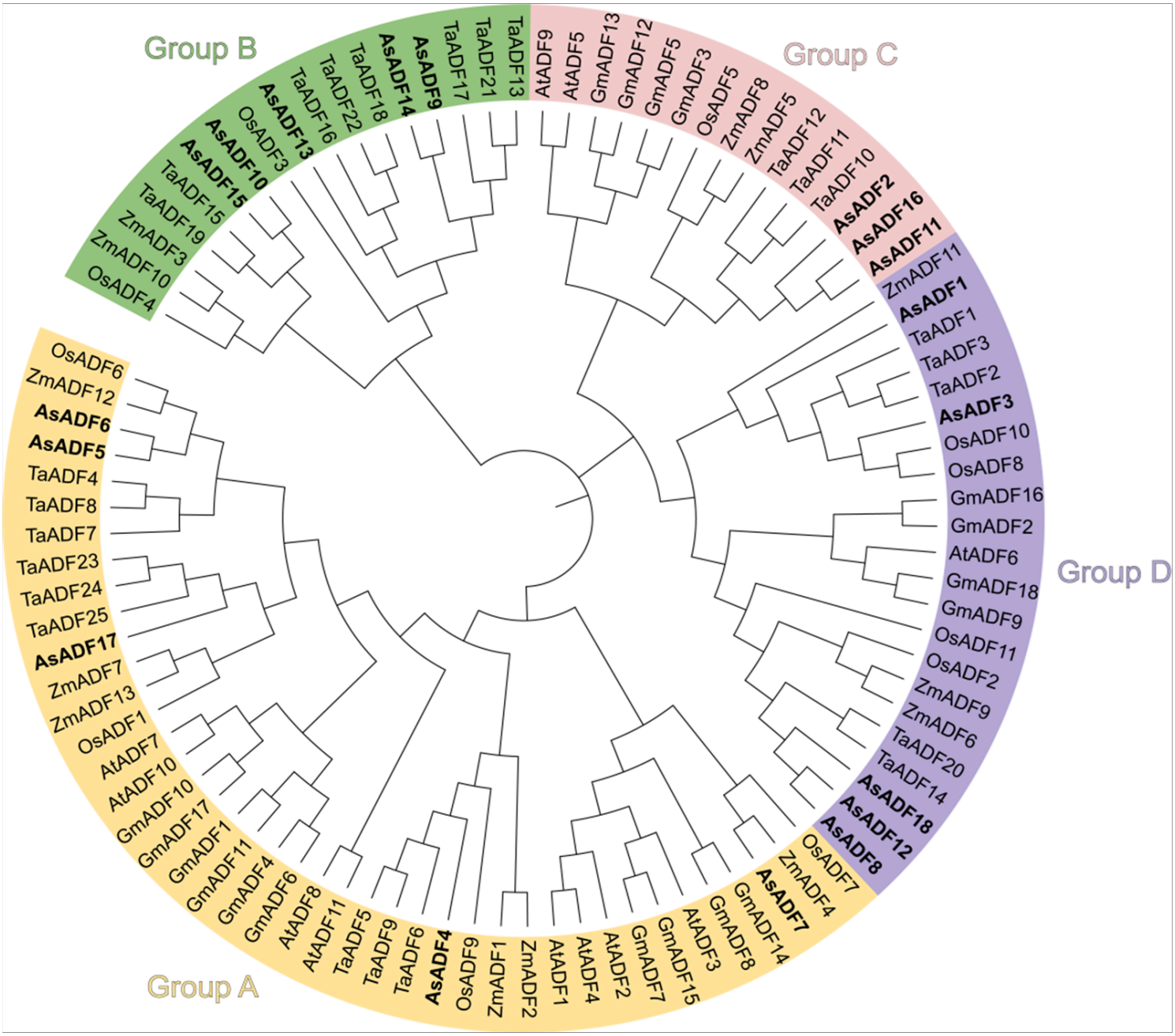

Figure 4

Phylogenetic tree of ADF family.

The phylogenetic tree is divided into four groups (A, B, C, and D).

The background is shaded in yellow, green, pink, and purple for Group A, B, C, and D, respectively.

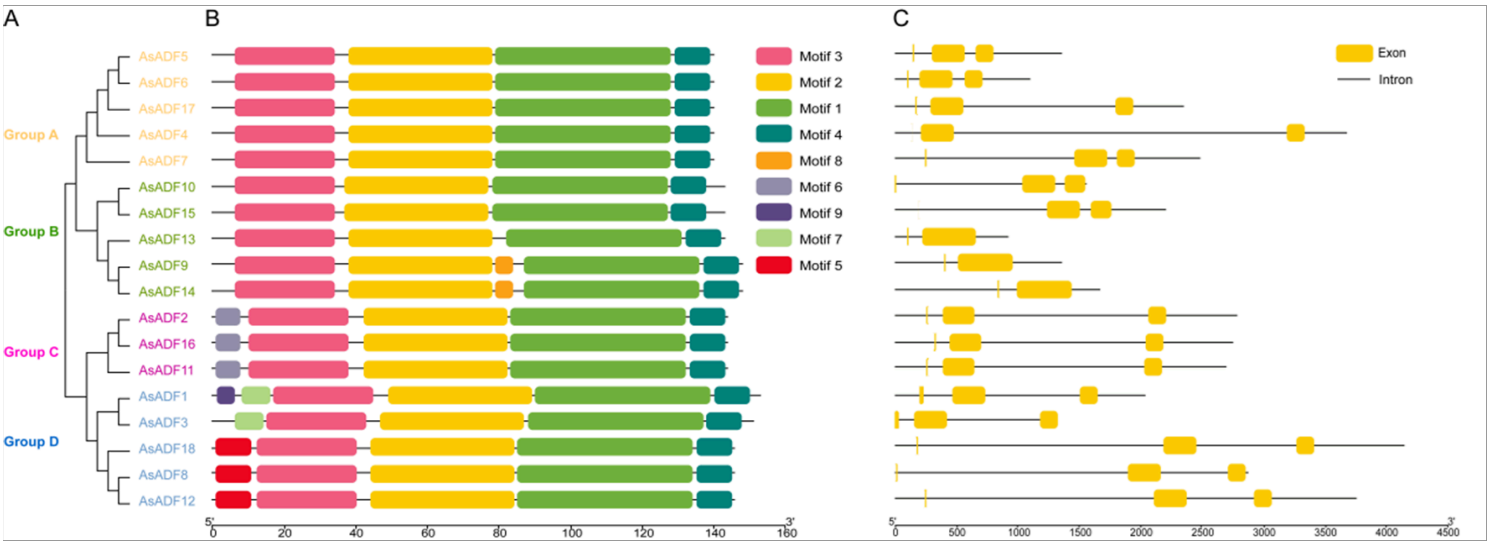

Figure 5

Phylogenetic analysis, conserved motifs, and gene structure of ADF proteins in oat.

(A) Phylogenetic tree of the oat ADF family constructed by the neighbor-joining method using MEGA software. (B) Distribution of conserved motifs in AsADF proteins. Different motifs are represented by numbered colored boxes. (C) Exon-intron structure of *AsADF*genes. Yellow boxes and black lines represent exons and introns, respectively.

The scale at the bottom applies to both panels (B) and (C).

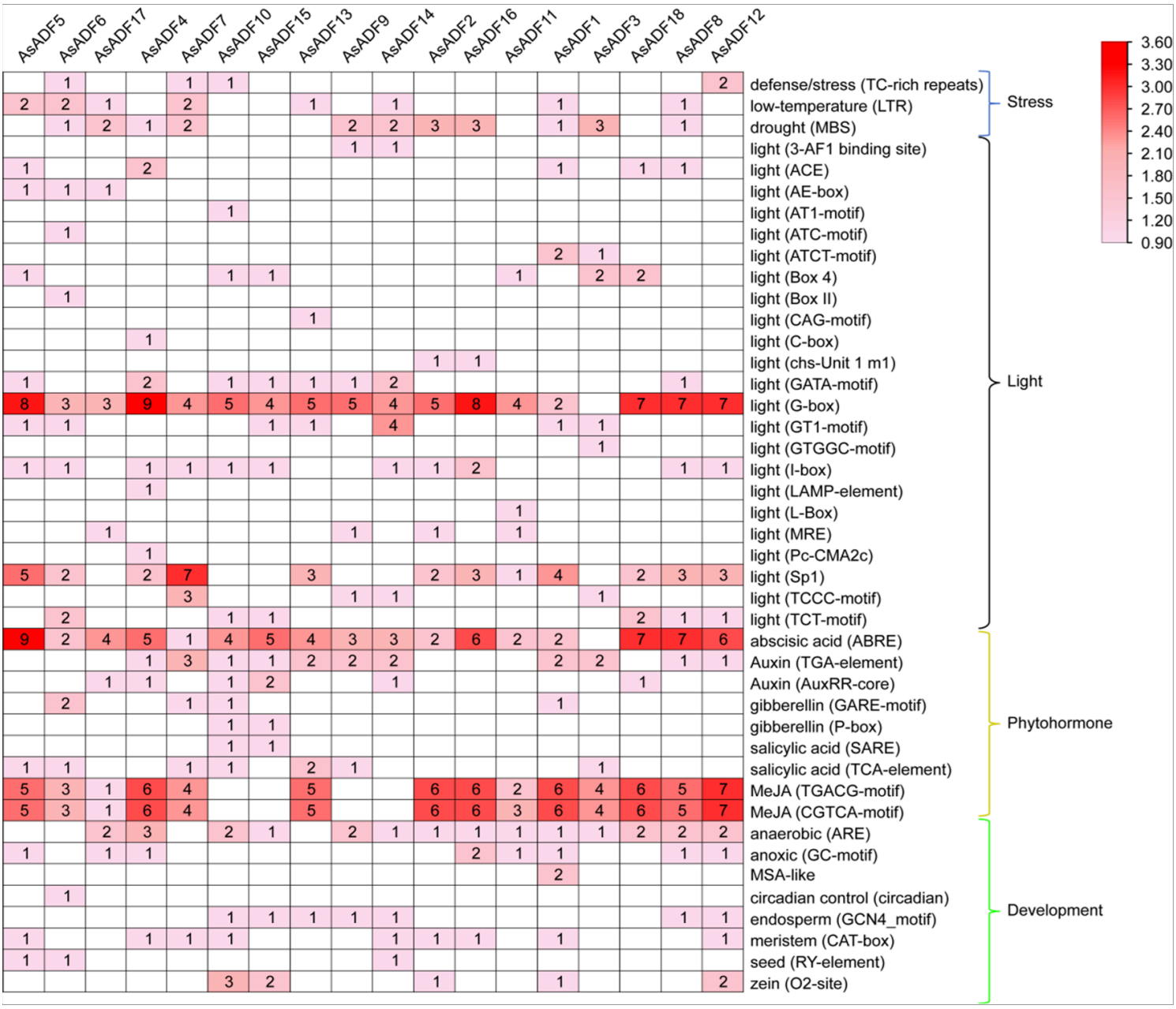

Figure 6

Prediction of promoter cis-elements.

The color scale from white to red indicates an increasing number of predicted elements.

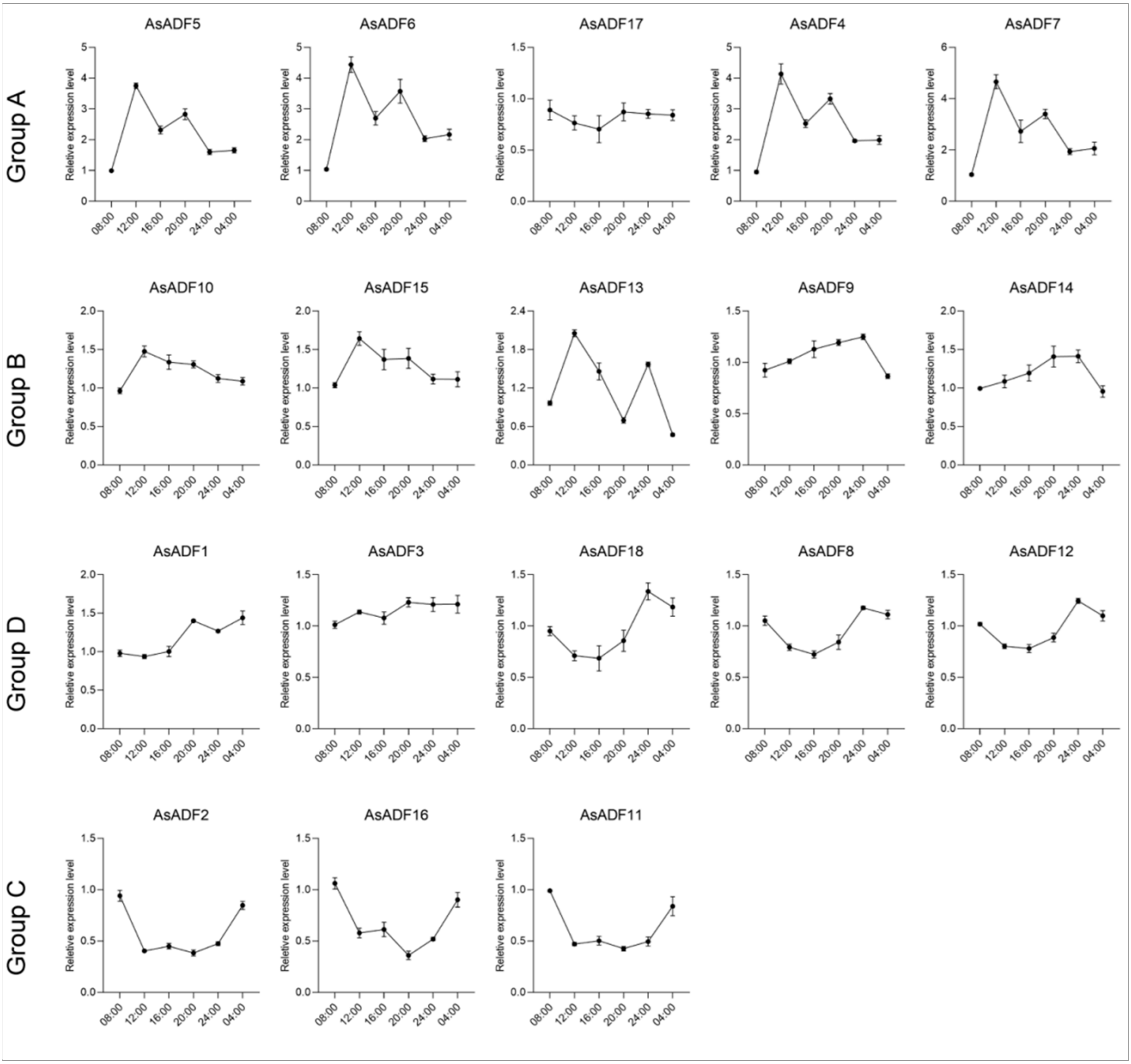

Figure 7

Circadian expression patterns of the *AsADF* gene family.

Relative expression levels were determined by qRT-PCR using *AsEIF4A* as an internal reference and calculated via the $2^{-\Delta\Delta Ct}$ method.

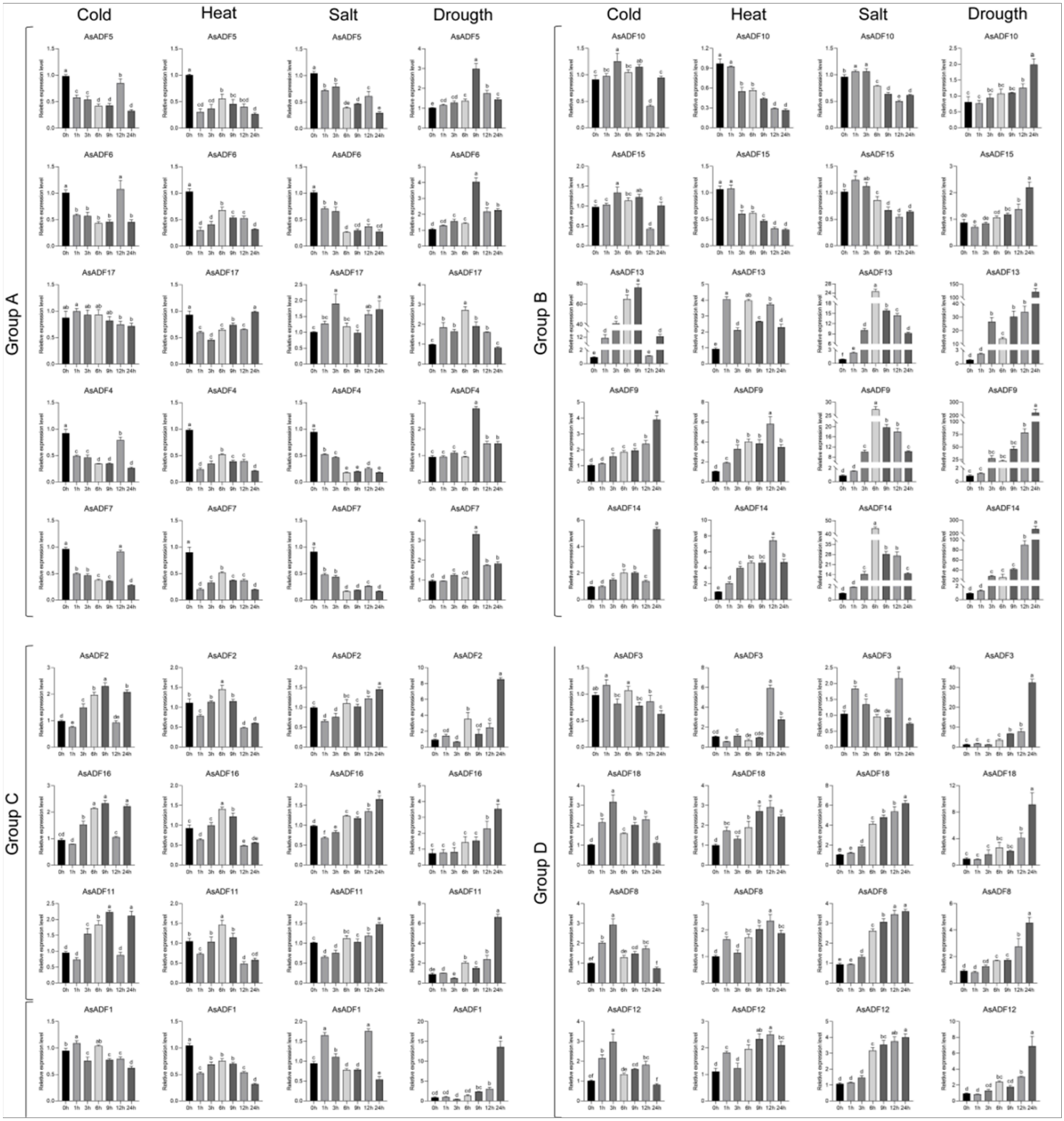

Figure 8

Expression patterns of 18 *AsADF* genes under cold, heat, salt, and drought stress in oat.

Relative expression levels were determined by qRT-PCR using *AsEIF4A* as an internal reference and calculated via the $2^{-\Delta\Delta Ct}$ method. Lowercase letters indicate statistically significant differences ($P < 0.01$) among time points within each treatment as determined by Tukey's test.

Supplementary Files

This is a list of supplementary files associated with this preprint. Click to download.

- Supplementarymaterial.rar